Myo10 in brain: developmental regulation, identification of a headless isoform and dynamics in neurons

Aurea D. Sousa*, Jonathan S. Berg*, Brian W. Robertson, Rick B. Meeker and Richard E. Cheney‡

Department of Cell and Molecular Physiology, Medical Biomolecular Research Building (MBRB), University of North Carolina at Chapel Hill, Chapel Hill, NC 27599-7545, USA

*These authors contributed equally to this work
‡Author for correspondence (e-mail: CheneyR@med.UNC.edu)

Summary

Although Myo10 (myosin-X) is an unconventional myosin associated with filopodia, little is known about its isoforms and roles in the nervous system. We report here that, in addition to full-length Myo10, brain expresses a shorter form of Myo10 that lacks a myosin head domain. This 'headless' Myo10 is thus unable to function as a molecular motor, but is otherwise identical to full-length Myo10 and, like it, contains three pleckstrin homology (PH) domains, a myosin-tail homology 4 (MyTH4) domain, and a band-4.1/ezrin/radixin/moesin (FERM) domain. Immunoblotting demonstrates that both full-length and headless Myo10 exhibit dramatic developmental regulation in mouse brain. Immunofluorescence with an antibody that detects both isoforms demonstrates that Myo10 is expressed in neurons, such as Purkinje cells, as well as non-neuronal cells, such as astrocytes and ependymal cells. CAD cells, a neuronal cell line, express both full-length and headless Myo10, and this endogenous Myo10 is present in cell bodies, neurites, growth cones and the tips of filopodia. To investigate the dynamics of the two forms of Myo10 in neurons, CAD cells were transfected with GFP constructs corresponding to full-length or headless Myo10. Only full-length Myo10 localizes to filopodial tips and undergoes intrafilopodial motility, demonstrating that the motor domain is necessary for these activities. Live cell imaging also reveals that full-length Myo10 localizes to the tips of neuronal filopodia as they explore and interact with their surroundings, suggesting that this myosin has a role in neuronal actin dynamics.

Introduction

The development of the nervous system involves numerous processes associated with cell motility and the cytoskeleton such as neuronal migration, growth cone crawling and extension of filopodia. Although myosins have been widely hypothesized to be involved in these processes (Jay, 2000; Mitchison and Kirschner, 1988; Smith, 1988; Suter and Forscher, 2000), their identities and roles are not yet clear. Myo10 (myosin-X) is a recently discovered myosin that localizes to the tips of filopodia, undergoes a novel form of motility within filopodia and leads to increased filopodia when overexpressed (Berg and Cheney, 2002; Sousa and Cheney, 2005). Little is known about Myo10 in brain or neurons, although its mRNA has been reported to increase sevenfold during nerve regeneration (Tanabe et al., 2003). Myo10 also binds to several molecules known to be important in neuronal development, including calmodulin (Homma et al., 2001), phosphatidylinositol (3,4,5)-trisphosphate [PtdIns(3,4,5)P_3] (Isakoff et al., 1998), microtubules (Weber et al., 2004), and β-integrins (Zhang et al., 2004). Although these properties suggest that Myo10 has important roles in the nervous system, the initial northern and immunoblots for Myo10 indicated that

brain expresses an uncharacterized, short form of Myo10 (Berg et al., 2000). Determining the nature of this short form of Myo10 is thus an essential first step in investigating Myo10's role in neurons; we report here the identity of this isoform as well as the developmental regulation, localization and dynamics of Myo10 in brain and neurons.

Myo10 is a vertebrate-specific member of a superclass of myosins, whose tails are characterized by the presence of myosin tail homology 4 (MyTH4) and band-4.1/ezrin/radixin/moesin (FERM) domains (Berg et al., 2001; Sousa and Cheney, 2005). MyTH-FERM myosins appear to mediate membrane-cytoskeleton interactions underlying processes such as adhesion (Tuxworth et al., 2001; Zhang et al., 2004), phagocytosis (Cox et al., 2002; Titus, 1999), and formation of filopodia and related structures (Belyantseva et al., 2003; Berg and Cheney, 2002; Tuxworth et al., 2001). Although Myo10 is expressed at relatively low levels, it appears to be the MyTH-FERM myosin expressed in most vertebrate cells (Berg et al., 2000).

The approximately 240 kDa heavy-chain of full-length Myo10 can be divided into head, neck and tail (Berg et al., 2000; Yonezawa et al., 2000). The head binds to actin,

hydrolyzes ATP and moves towards the barbed end of the actin filament (Homma et al., 2001). The neck consists of three IQ motifs, each of which provides a binding site for calmodulin or a calmodulin-like light-chain (Homma et al., 2001; Rogers and Strehler, 2001). The tail begins with a segment predicted to form a coiled coil, which suggests that the Myo10 heavy-chains can dimerize. The coiled coil is followed by three PEST (proline-, glutamate-, serine- and threonine-rich) regions that provide proteolytic cleavage sites and may allow the motor to be decoupled from the remainder of the tail (Berg et al., 2000). The Myo10 tail is unique among myosins because it includes three pleckstrin homology (PH) domains and can bind PtdIns(3,4,5)P_3 (Isakoff et al., 1998; Mashanov et al., 2004). This suggests that Myo10 functions downstream of phosphoinositide 3-kinase (PI 3-kinase), an important regulator of cell motility. The Myo10 tail also includes a MyTH4 domain that can bind to microtubules, thus allowing Myo10 to link actin filaments and microtubules (Weber et al., 2004). The Myo10 heavy-chain ends in a FERM domain that can bind to the cytoplasmic domain of β_1-, β_3- or β_5-integrin (Zhang et al., 2004), which suggests Myo10 can act as a motorized clutch to link cell adhesion molecules to the actin cytoskeleton.

Myo10 exhibits a striking localization to the tips of the slender actin-based extensions known as filopodia (Berg and Cheney, 2002; Berg et al., 2000). Filopodia appear to act as cellular sensors in processes such as growth cone guidance (Davenport et al., 1993), angiogenesis (Gerhardt et al., 2003) and cell migration (Rorth, 2003). Filopodia contain a core of bundled actin filaments and are surrounded by a cylindrical sheath of plasma membrane (Svitkina et al., 2003). Actin polymerization occurs at the barbed ends of the actin filaments, which are located at the tip of the filopodium. Since the actin filaments in filopodia undergo retrograde (rearward) flow, it is the balance between the rate of actin polymerization at the filopodial tip and the rate of retrograde flow that determines whether a given filopodium extends or retracts (Mallavarapu and Mitchison, 1999). In addition to localizing at the tips of filopodia, full-length Myo10 undergoes forward and rearward movements within filopodia that we term intrafilopodial motility (Berg and Cheney, 2002). We hypothesize that the forward movements are powered by the Myo10 motor domain moving towards the barbed ends of filopodial actin filaments, whereas the rearward movements result from a rigor-like binding to actin filaments that undergo retrograde flow. Full-length Myo10 can also stimulate the formation or stabilization of filopodia because, when overexpressed, it increases the number and length of filopodia in COS-7 cells (Berg and Cheney, 2002). This effect is not observed with an HMM-like Myo10 construct or a tail-alone construct (Berg and Cheney, 2002).

We report here that, brain and neuronal cells express a headless form of Myo10, which lacks nearly all of the myosin motor domain, and is thus unable to function as a molecular motor. We also show that both full-length and headless Myo10 exhibit dramatic developmental regulation in brain. In addition, we report the first immunolocalization of Myo10 in brain, and use CAD cells as a model system to investigate the dynamics of headless and full-length Myo10 in a neuronal cell line. These experiments reveal that although headless Myo10 does not localize to neuronal filopodia or undergo intrafilopodial motility, full-length Myo10 does localize to the tips of filopodia and can undergo several intriguing forms of motility in neuronal cells.

Results
Identification of a headless myosin in brain
Although previous research indicated that brain expresses a short form of Myo10, the structure of this short form was unknown (Berg et al., 2000). A human multiple tissue northern blot, probed with sequences consisting primarily of 3′ UTR from full-length Myo10, indicated that the short form of Myo10 expressed in brain is ~2 kb shorter than the full-length (~9 kb) mRNA expressed in other tissues (Berg et al., 2000) (Fig. 1). Immunoblots of bovine tissues were consistent with this finding and indicated that the short form in brain is ~60-70 kDa smaller than the ~240 kDa full-length Myo10 (Berg et al., 2000) (Fig. 2) The short form reacted with two different antibodies to bovine Myo10, one made against amino acids (aa) 1-952 and another against aa 1639-1798. The short form of Myo10 is thus expected to include a sequence from both these regions as well as a sequence from the 3′ UTR, while being ~60-70 kDa smaller than full-length Myo10.

To determine the structure of the short form of Myo10, we first generated an intron-exon map of the human *MYO10* gene by aligning a full-length human *MYO10* cDNA (NM_012334) with genomic sequence (Fig. 1A). We then searched the National Center for Biotechnology Information (NCBI) database to identify expressed sequences tags (ESTs), potentially encoding the short form of Myo10. We found a human EST from fetal brain [gi:5552940/AI878891; nucleotide (nt) 191-568] that matched perfectly with nt 2152-2529 of the full-length *MYO10* cDNA. The matching sequence is located at the start of the *MYO10* exon that begins with M_{644}. However, the first part of the EST (nt 34-190) did not match this region but instead matched perfectly with a genomic sequence for the full-length transcript, located ~30 kb upstream of the exon encoding M_{644} in the middle of a very large (~43 kb) intron. This suggests that, the short form of Myo10 results from the use of an alternative promotor, which transcribes an alternative exon encoding a 5′ UTR unique to the short form. This 5′ UTR is spliced to the exon beginning with M_{644}, a methionine predicted by GENSCAN to function as a translation start site (Burge and Karlin, 1997). Since this short transcript would lack most of the Myo10 motor domain but include the rest of Myo10 (aa 644-2058), we refer to it as headless Myo10. Consistent with the data obtained from northern blots, the headless Myo10 transcript shares the same 3′ UTR as the full-length Myo10, but is ~2 kb shorter. Consistent with previous immunoblotting data, translation that starts at M_{644} results in a protein of 163,567 Da (1415 aa), which overlaps with both of the fusion protein constructs that were used to make the initial antibodies against Myo10.

Northern blot and PCR evidence for the headless Myo10 transcript
To test whether the short form of Myo10 observed in northern blots corresponds to this headless transcript, we reprobed the human-multiple-tissue northern blot with the 5′ UTR specific to the headless form. As predicted, this probe detected the short (~7 kb) *MYO10* transcript but not the
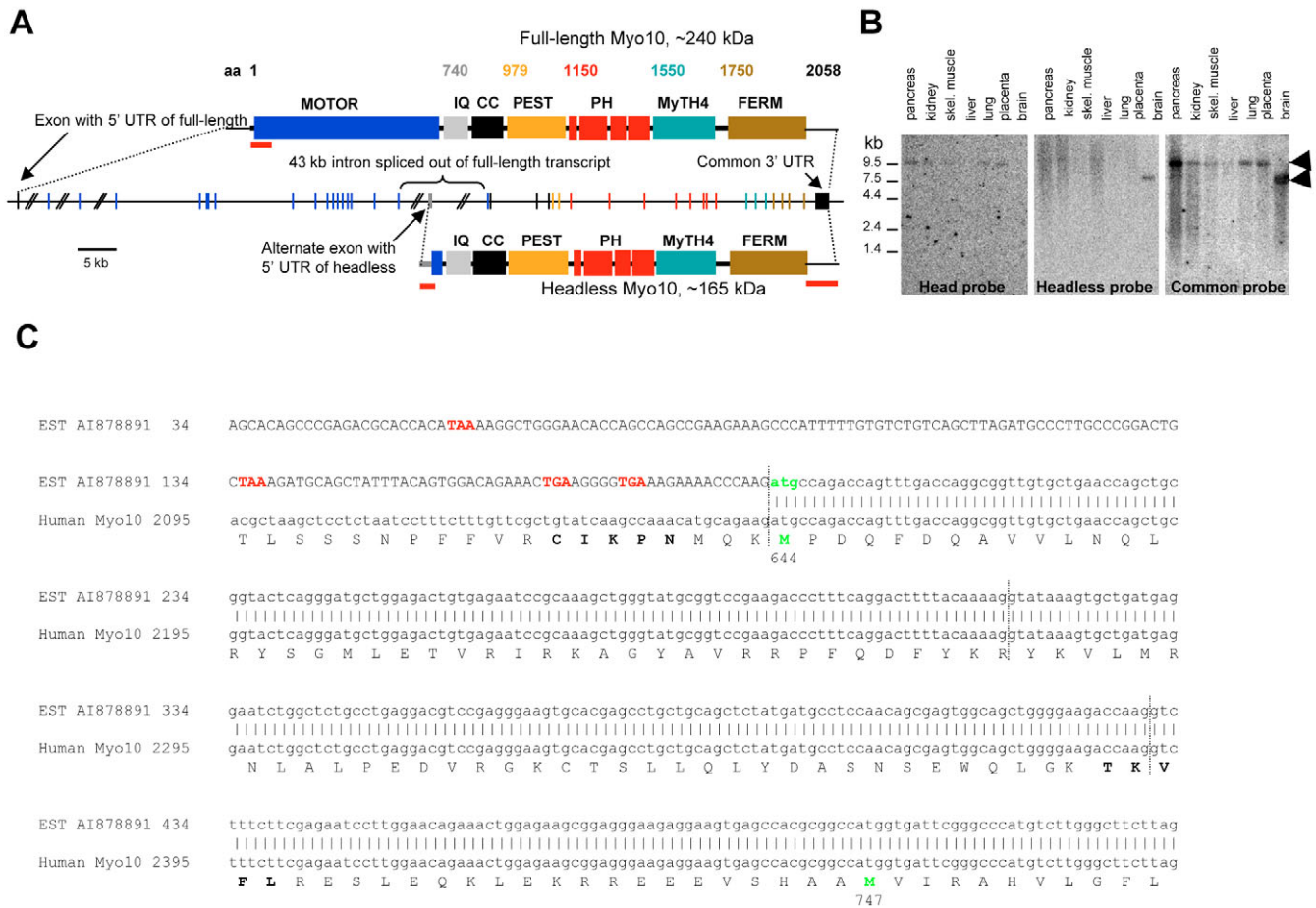
Fig. 1. Brain expresses a headless form of Myo10. (A) Schematic map of the human Myo10 gene and bar diagrams of the full-length and headless Myo10 transcripts. The headless transcript begins with an alternate exon (gray) that encodes a 5′ UTR specific to headless Myo10. Splicing of this 5′ UTR to the exon that begins at M644 of full-length Myo10, results in a headless transcript lacking the first 643 aa of full-length Myo10. Major domains of the Myo10 protein are indicated by colored boxes, vertical lines on the gene map represent exons. The horizontal red lines indicate the locations of the probes used for northern blotting. (B) Multiple-tissue northern blot incubated with three different Myo10 probes. The blot was originally incubated with a probe targeting the 3′ UTR common to both transcripts (right) and detected both a ~9 kb band (upper arrowhead) in non-brain tissues and a smaller ~7 kb band (lower arrowhead) in brain (Berg et al., 2000). The blot was then stripped and reprobed with a sequence from the 5′ UTR of the headless transcript (middle), which detected a ~7 kb band in brain but not the full-length ~9 kb band in other tissues. The blot was then stripped and reprobed a final time with a sequence from the head domain (left). In addition to the ~7 kb band in brain, the headless probe appears to react non-specifically with a faint band in tissues such as liver that is slightly larger than the ~9 kb band corresponding to full-length Myo10. (C) Sequence alignment of human EST AI878891 with full-length Myo10 cDNA (NM_012334) show the 5′ UTR specific to the headless form (capitalized nucleotides) as well as the initial protein-coding exons of the headless form and their perfect match to the full-length Myo10 exon beginning at M644. Exon boundaries are indicated by vertical dotted lines and stop codons in the alternate 5′ UTR are highlighted in red. Predicted start methionines at M644 and M747 are shown in green.

larger (~9 kb) full-length transcript (Fig. 1). In addition, when the blot was reprobed with a sequence from the head domain, we detected only the full-length (~9 kb) band and not the shorter transcript. To further confirm the existence of headless Myo10, we performed PCR of brain cDNA with a forward primer specific for the 5′ UTR of the headless transcript and a reverse primer from an exon that is shared by both transcripts. These primers would be 377 nt apart in the headless but are ~33,000 nt apart in genomic sequence. As expected from transcription of headless Myo10, a band of ~377 nt was amplified. Cloning and sequencing of this PCR product showed that it perfectly matches the 5′ UTR and the coding sequence predicted for headless Myo10.

Additional EST evidence for headless Myo10 in human and mouse

Recent database searches have revealed at least eight additional human ESTs that correspond to the headless Myo10 transcript [gi:52240826 and gi:52278375 from brain, gi:52103381 from fetal brain, gi:52087137 from corpus callosum, gi:52194716 and gi52191621 from the glioma cell line KG-1-C, gi:24044427 from a teratocarcinoma cell line, and gi:47334466 from embryonic stem (ES) cells]. The initial, automated analysis of the mouse genome also predicted the existence of an equivalent transcript for headless Myo10 in mouse (sequence record XM_192774), and there are at least six mouse ESTs that correspond to the 5′ UTR and initial coding sequence of the headless Myo10 transcript [gi:34584306 from

newborn brain, gi:26467095 from visual cortex, gi:29353457 from prenatal brain, gi:22497702 from embryonic day 12.5 (E12.5) whole brain, gi:16458330 from whole E8 embryo, and gi:27328064 from neuronal stem cells]. Finally, analysis of the Riken full-length enriched cDNA collection indicates that the mouse clone ri:5730439K04 from E8 mouse embryo has a 5′-sequence-read (PXB0064413a/BB618862) that perfectly matches the first ~500 nt of the predicted headless transcript and a 3′-sequence-read (PXB00644K13b/AV296136) that perfectly matches ~600 nt of the 3′ UTR shared by both full-length and headless Myo10. Together, these data from sequence analysis, northern blotting, PCR and immunoblotting thus demonstrate the existence of headless Myo10 in both human and mouse brain.

Headless and full-length Myo10 are developmentally regulated in brain

To determine whether Myo10 is developmentally regulated, we generated an antibody (no. 3568) to the coiled-coil region of mouse Myo10, and used it to blot samples from the cerebri and cerebelli of mice, ranging in age from postnatal day 1 (P1) to adult. Since the headless transcript contains the coiled-coil region, this antibody was predicted to react with both full-length and headless Myo10. As expected, the new antibody reacted with the ~240 kDa full-length and the ~165 kDa short form in immunoblots of mouse brain (Fig. 2). In the mouse cerebrum, Myo10 exhibited striking developmental regulation, with both forms showing a peak of expression between P5 and P15, and greatly decreased expression in the adult. A different pattern of expression was observed in the mouse cerebellum, where full-length Myo10 was expressed much more

prominently than the short form. In addition, expression of full-length Myo10 continued to increase during postnatal development of the mouse cerebellum, with adult cerebellum exhibiting the highest level of expression.

Myo10 is expressed in neurons and non-neuronal cells

Although brain clearly expresses both full-length and headless Myo10, there was no data on the immunolocalization of Myo10 in brain and it was not clear whether Myo10 is expressed in both neurons and glia or whether it localizes selectively to axons as opposed to dendrites. We therefore performed immunofluorescence localization experiments on frozen sections of mouse brain with the new antibody against mouse Myo10. In adult mouse cerebellum, the brightest staining for Myo10 was observed in the cell bodies and dendrites of Purkinje cells (Fig. 3A-F), consistent with our previous data from in-situ hybridization (Berg et al., 2000). In optimally oriented sections, faint staining of Purkinje-cell axons was sometimes observed (not shown). In general, however, white matter showed relatively little Myo10 staining (Fig. 3A). The Myo10 antibody also stained the processes of glial cells, such as the Bergmann glia, as shown by double labeling with the astrocytic marker glial fibrillary acidic protein (GFAP) (Fig. 3G-L). Although antibody no. 3568 detects both full-length and headless Myo10 in immunoblots, it is likely that the immunostaining in adult mouse cerebellum is due to full-length Myo10, because this is the only form that was detected in immunoblots of adult mouse cerebellum (Fig. 2B). Consistent with the relatively low level of Myo10 expression detected in immunoblots of adult mouse cerebrum, only faint Myo10 staining was observed in the parenchyma of this tissue (not shown). Sections from cerebrum that included the ventricles, however, revealed that Myo10 stains ependymal cells brightly (Fig. 3M). These cells form a single layer of epithelial cells that line the ventricles and are of special interest because they have been suggested to function as neuronal stem cells (Johansson et al., 1999). The astrocytes subjacent to the ependymal cells also show some Myo10 staining, as shown by the colocalization with GFAP (Fig. 3N,O). Brain sections incubated with a non-immune control generated little or no background-staining under these conditions (data not shown).

Both isoforms of Myo10 are expressed in CAD cells

To investigate the localization and dynamics of Myo10 in neurons, we used CAD cells as a neuronal cell culture model. CAD cells are a transfectable mouse cell line that can be induced to differentiate into catecholaminergic neurons by serum withdrawal (Qi et al., 1997). To determine whether CAD cells express endogenous Myo10, we first immunoblotted SDS lysates of CAD cells with the antibody against mouse Myo10. Consistent with the widespread expression of full-length Myo10 in mammalian cells, the band of the ~240 kDa full-length Myo10 was detected in both undifferentiated and differentiated CAD cells (Fig. 2C). The band of the ~165 kDa headless Myo10 was also detected in both types of CAD cells. Similar results were obtained in immunoblotting experiments with other cell lines that can be differentiated into a neuronal phenotype such as PC-12 pheochromocytoma cells and B35 neuroblastoma cells (data not shown), suggesting that headless Myo10 is expressed at very early stages of neuronal development.
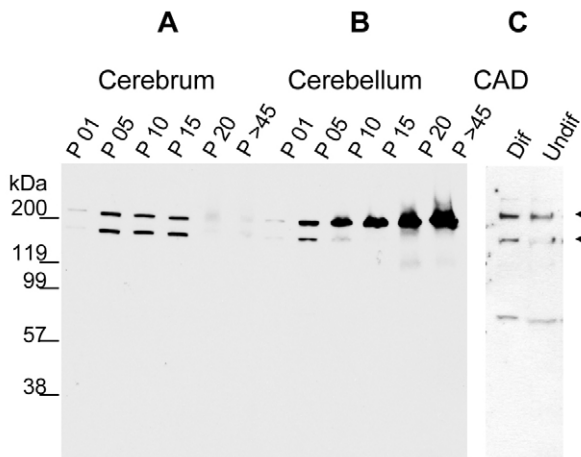

Fig. 2. Myo10 expression in brain is developmentally regulated. Western blot of whole cerebri (A) or cerebelli (B) from mice at postnatal days 1 to adult (*P*>45) were lysed in SDS sample buffer and immunoblotted with antibody no. 3568 against mouse Myo10. Both full-length- (~240 kDa) and headless-Myo10 (~164 kDa) are expressed in mouse cerebrum where they show clear developmental regulation, with a peak of expression between postnatal days 5-15. Cerebellum from mouse shows a different pattern of Myo10 expression, with prominent and increasing levels of full-length Myo10 expression throughout development. (C) Full-length and headless Myo10 (arrowheads) are detected by immunoblotting in undifferentiated CAD cells as well as in CAD cells differentiated into a neuronal phenotype.

Fig. 3. Immunolocalization of Myo10 in mouse brain. (A-C) Sagittal section from the cerebellum of an adult mouse double-labeled for Myo10 and calbindin, a marker for Purkinje cells. The cell bodies of Purkinje cells (PL) and their dendrites in the molecular layer (ML) are brightly stained by Myo10. Myo10 stains the granule-cell layer (GL) more faintly, and the cerebellar white matter (WM) shows little staining. (D-F) A similar section of the molecular layer at higher magnification shows staining for Myo10 in the dendrite (arrow in E) of a Purkinje cell. (G-I) Sagittal section from the cerebellum of an adult mouse double-labeled for Myo10 and GFAP, a marker for Bergmann glia and other astrocytes. (J-L) A similar section of the molecular layer at higher magnification showing that Myo10 staining is also present in the processes of Bergmann glia (arrow in K). (M-O) Sagittal section from the cerebrum of an adult mouse double-labeled for Myo10 and GFAP showing staining of the ventricular zone (VZ) and subventricular zone (SVZ). Although the parenchyma of the adult mouse cerebrum shows relatively faint Myo10 staining, the ependymal cells lining the ventricle show bright Myo10 staining. The subjacent subventricular astrocytes marked by GFAP staining (red arrow in H) are also Myo10 immunopositive.
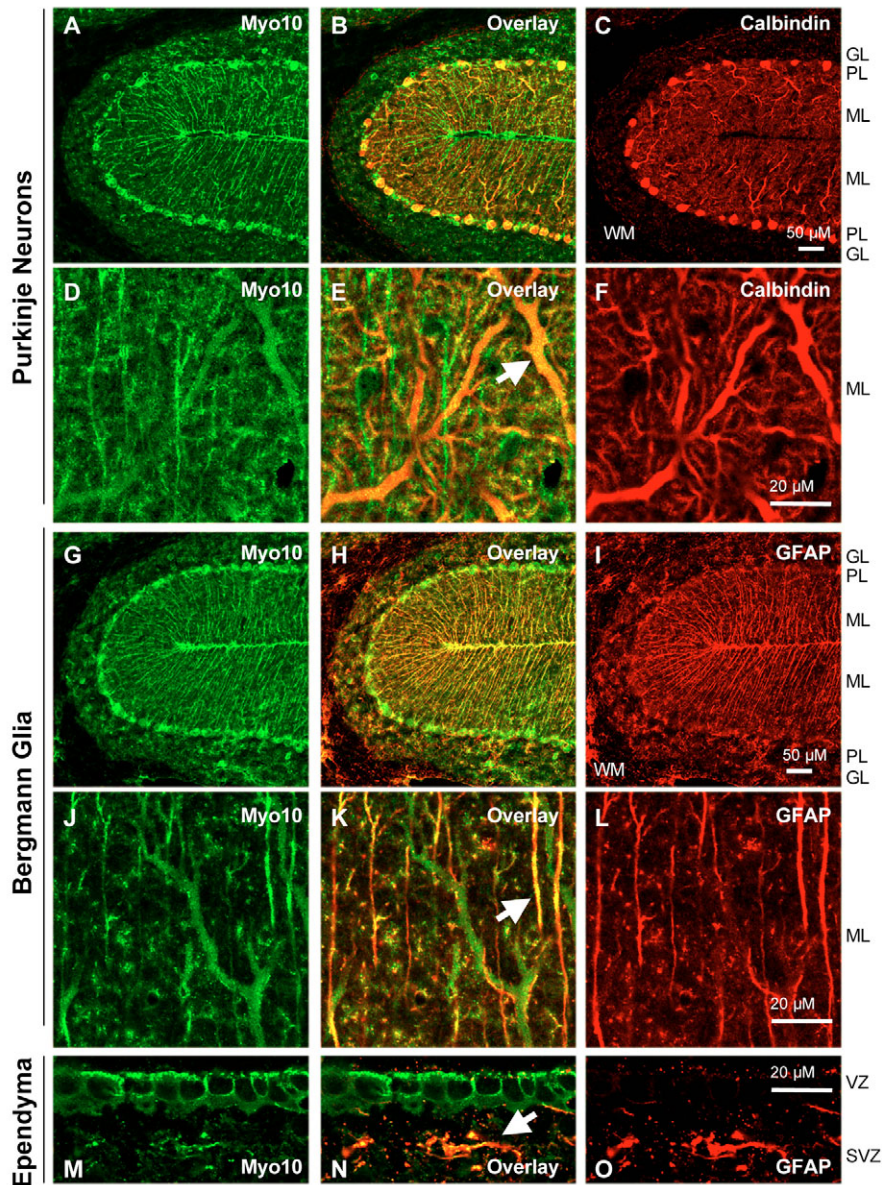
Undifferentiated CAD cells form prominent lamellipodia with short filopodia along their leading edge (Fig. 4A,B). These filopodia give rise to large bundles of actin or 'rootlets' that extend deep into the lamellipodium. CAD cells thus have an actin organization somewhat similar to that of growth cones from *Aplysia* (Lin et al., 1997) and *Helisoma* (Zhou et al., 2002). CAD cells differentiated by serum withdrawal for ~2 days acquire a neuronal phenotype and form neurites, growth cones, and numerous long filopodia (Fig. 4C,D). Immunostaining in undifferentiated CAD cells with antibody no. 3568 revealed that endogenous Myo10 localizes at the tips of short filopodia but is also present at the plasma membrane and cell body (Fig. 4A). In differentiated CAD cells, endogenous Myo10 clearly localizes at the tips of neuronal filopodia, but also exhibits a more diffuse localization in neurites and cell bodies (Fig. 4C). A similar pattern of localization was seen in cultured primary rat neurons (supplementary material, Fig. S1). Control cells stained with non-immune IgG show little or no background under these staining conditions (Fig. 4B,D).

Full-length, but not headless Myo10, localizes to the tips of neuronal filopodia

Although the experiments described above revealed the subcellular localization of endogenous Myo10 in neurons, they did not allow us to distinguish between the localization of headless and full-length Myo10 because the antibody reacts with both forms. To investigate the functional differences between these two forms of Myo10, we expressed GFP constructs corresponding to full-length and headless Myo10 in CAD cells. In undifferentiated CAD cells, full-length GFP-Myo10 localizes to the tips of the short filopodia at the edge of the lamella (Fig. 5A). Headless GFP-Myo10 does not localize to filopodial tips and instead exhibits a more diffuse localization to the lamellipodial plasma membrane and cell body (Fig. 5B).

In differentiated CAD cells, full-length GFP-Myo10 localizes to the tips of neuronal filopodia, although it is also present in neurites and cell bodies (Fig. 5C). Headless GFP-Myo10 does not localize to the tips of neuronal filopodia, and instead exhibits a more diffuse localization along neurites and cell bodies (Fig. 5D). The localization of full-length GFP-Myo10 to the tips of filopodia is particularly striking at early stages of differentiation, when numerous filopodia are present (Fig. 5E). It should also be noticed that GFP-Myo10 localizes
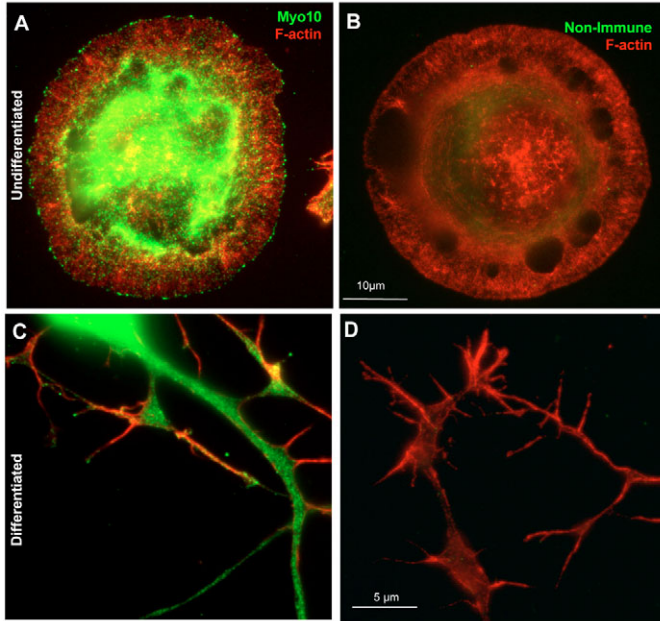
Fig. 4. Subcellular localization of endogenous Myo10 in CAD cells. (A) In undifferentiated CAD cells, Myo10 shows a clear localization to the leading edge as well as a more diffuse localization in central cytoplasm. (B) Undifferentiated CAD cells stained with a non-immune control antibody show little or no staining. (C) After ~2 days of serum withdrawal to induce CAD-cell differentiation into a neuronal phenotype, Myo10 staining is observed in cell bodies, neurites, the edges of growth cones and the tips of neuronal filopodia. (D) Differentiated CAD cells stained with a non-immune control antibody show little or no staining. Myo10 antibody no. 3568 was used to stain Myo10 (green) and rhodamine-phalloidin was used to label F-actin (red).

to the tips of filopodia-like structures at sites of cell-cell contact in both undifferentiated (Fig. 6A) and differentiated CAD cells (Fig. 6B; see also supplementary material Movie 5).

Live-cell imaging of Myo10 dynamics in undifferentiated CAD cells

To simultaneously visualize the dynamics of actin and Myo10, undifferentiated CAD cells were transfected with CFP-β-actin and GFP-Myo10. As seen in Figs 4-6, undifferentiated CAD cells have a lamellipodial morphology quite different from the HeLa cells used in our previous live-cell imaging experiments (Berg and Cheney, 2002). Like growth cones, the lamellipodia of these cells exhibit prominent retrograde flow (supplementary material, Movies 1, 2). As expected, live-cell imaging shows that both full-length Myo10 and the largely tailless HMM-Myo10 construct localize to the tips of filopodia. Live-cell imaging also reveals that the tip puncta formed by these constructs are occasionally 'released' from the tip and move rearward through the lamellipodium, a behavior that was especially prominent with HMM-Myo10 (supplementary material, Movie 1). These movements demonstrate for the first time that puncta of Myo10 are able to move rearward within lamellipodia along filopodial 'rootlets'. GFP-Myo10 moved rearward at the same rate as the CFP-actin, consistent with the hypothesis that rearward movement of Myo10 results from its binding to actin filaments
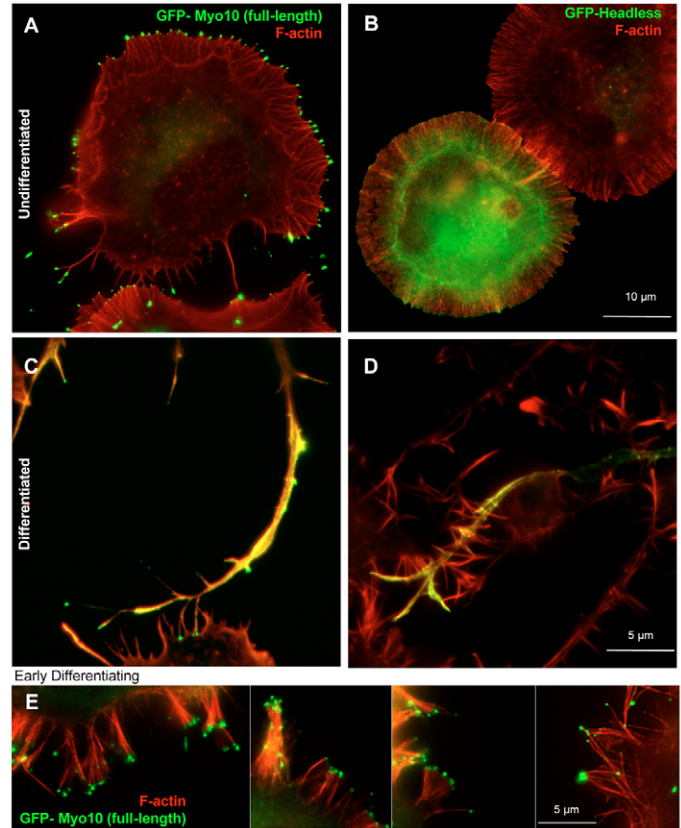

Fig. 5. Full-length Myo10, but not headless Myo10, localizes to the tips of filopodia when transfected into CAD cells. (A) In undifferentiated CAD cells, full-length GFP-Myo10 (green) localizes to the tips of the short filopodia along the leading edge. (B) Headless GFP-Myo10 does not localize to filopodial tips and instead shows a more diffuse localization to the cell membrane and the central portion of undifferentiated CAD cells. (C) In CAD cells induced to differentiate into a neuronal phenotype, full-length GFP-Myo10 localizes to neurites as well as the tips of neuronal filopodia. (D) Headless GFP-Myo10 localizes primarily to the soma and neurites of differentiated CAD cells and does not localize to the tips of filopodia. (E) High-magnification images showing localization of full-length GFP-Myo10 to the tips of filopodia in CAD cells at early stages of differentiation. Notice that the filopodia frequently clump together at their tips. Cells were double-labeled with rhodamine-phalloidin to stain F-actin (red).

that are undergoing retrograde flow. The observation that HMM-Myo10 exhibits localization and movements similar to those of full-length Myo10 also supports this model. Headless Myo10 exhibits a relatively diffuse distribution and does not localize to filopodial tips or undergo intrafilopodial motility (supplementary material, Movie 2).

Myo10 can undergo lateral movements along the leading edge

In addition to radial movements along filopodial actin bundles, we also discovered that Myo10 tip puncta can undergo lateral movements along the leading edge of CAD cell lamellipodia. Interestingly, these lateral movements sometimes lead tip puncta to collide and fuse with other puncta along the leading edge. Lateral fusion events occasionally appeared to trigger
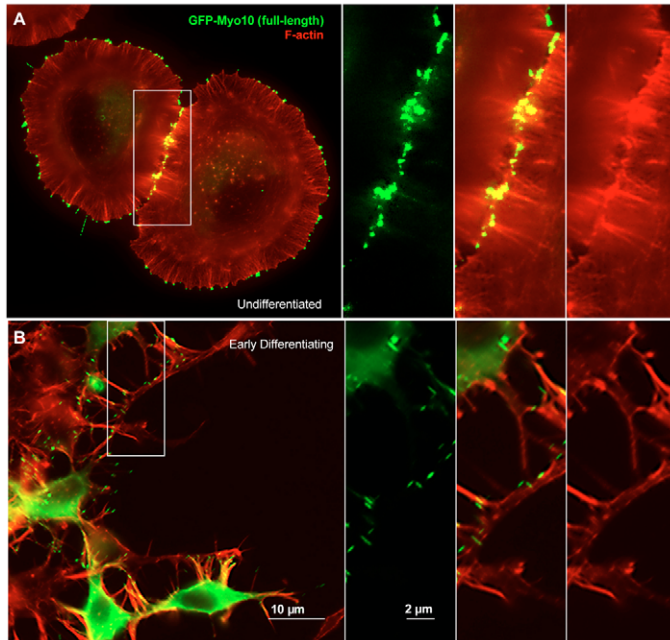
Fig. 6. Full-length Myo10 localizes to sites of cell-cell contact.
(A) In undifferentiated CAD cells, GFP-Myo10 (green) is present at
the tips of short filopodia-like structures at sites of cell-cell contact.
The panels on the right shows high-magnification views of the inset.
(B) GFP-Myo10 is also present at the tips of filopodia at sites of cell-
cell contact in differentiated CAD cells. The panels on the right show
high-magnification views of the inset and illustrate that Myo10 is
present at the tips of filopodia that are contacting neurites. Cells were
double-labeled for F-actin by staining with rhodamine-phalloidin
(red). Although under the exposure settings used here some filopodia
appear only faintly labeled for F-actin relative to the much thicker
neurites and cell bodies, longer exposures indicate that all of the
filopodia contain F-actin.

the tip puncta to move rearward, a behavior that was especially
prominent with HMM-Myo10 (supplementary material,
Movie 1). The lateral movements of small tip puncta and their
fusion with larger puncta are clearly illustrated by
kymographic analysis of the leading edge from a relatively

stationary CAD cell transfected with full-length GFP-Myo10
(Fig. 7; supplementary material, Movie 3). The dendritic
pattern of this kymograph demonstrates that, although the
larger tip puncta appear to be relatively stable, smaller tip
puncta continuously appear along the leading edge and move
laterally until they collide and fuse with brighter tip puncta.
This indicates that the leading edge is continuously generating
new tip puncta and that these move laterally until they fuse
with larger and apparently more stable tip puncta.

Dynamics of Myo10 in differentiating CAD cells
Full-length GFP-Myo10 also exhibits several intriguing
forms of movement in CAD cells differentiated to a more
neuronal phenotype. The lamellipodium of the transfected
CAD cell seen on the left side of Movie 4 in the
supplementary material, for example, shows several examples
of Myo10 tip puncta undergoing rearward movement in
lamellipodia. Although some of these rearward movements
are due to translocation of an entire filopodium, in other cases
puncta of Myo10 move rearward along a filopodial rootlet.
We also discovered that puncta of GFP-Myo10 occasionally
undergo 'rocketing' movements within the cell body. This is
seen most clearly with the very bright spot of GFP-Myo10 on
the left side of Movie 4 in the supplementary material. After
moving rearward, this spot of GFP-Myo10 spirals forward at
the tip of an actin-rich intrapodium. Other examples of
rocketing intrapodia with Myo10 at their tips can also be seen
in this region. GFP-Myo10 can also undergo both forward
and rearward intrafilopodial motility in neuronal filopodia
and retraction fibers (supplementary material, Movie 4).
Movie 5 in the supplementary material demonstrates that
GFP-Myo10 is present at the tips of neuronal filopodia when
they extend, retract and interact with a neurite from a
nontransfected cell. As expected, if the tip localization and
movements are due to Myo10 motor activity, the largely
tailless GFP-HMM-Myo10 construct exhibits similar tip
localization and movements (supplementary material, Movie
6). The very active dynamics of GFP-Myo10 in neuronal
filopodia on the cell body, neurite and growth cone are
illustrated in supplementary material Movie 7, where Myo10
is associated with numerous filopodia as they extend, retract
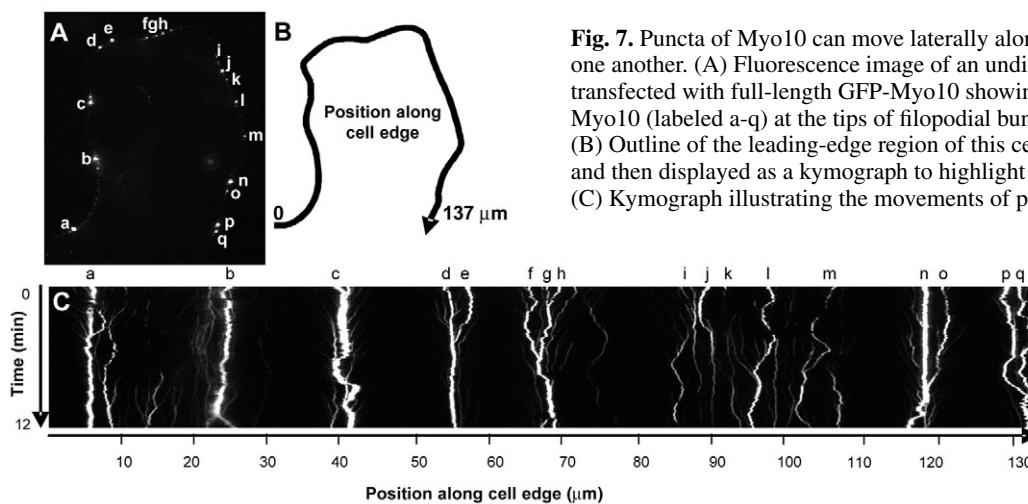and undergo intrafilopodial motility.

Fig. 7. Puncta of Myo10 can move laterally along the leading edge and fuse with
one another. (A) Fluorescence image of an undifferentiated CAD transiently
transfected with full-length GFP-Myo10 showing 17 relatively large puncta of GFP-
Myo10 (labeled a-q) at the tips of filopodial bundles along the leading edge.
(B) Outline of the leading-edge region of this cell that was imaged for 12 minutes
and then displayed as a kymograph to highlight movements along the lateral edge.
(C) Kymograph illustrating the movements of puncta of Myo10 along the leading
edge. Although the larger
Myo10 puncta maintained
relatively stable positions
along the leading edge,
smaller Myo10 puncta
tended to move laterally
along the leading edge until
they collided and fused with
larger puncta, thus
generating a kymograph
with a dendritic appearance.

Discussion

Discovery of a headless Myo10 in brain

The data presented here from sequence analysis, northern blots, PCR and immunoblots demonstrate that brain expresses a headless form of Myo10. Headless Myo10 thus lacks the defining element of a myosin and is unable to function as a molecular motor. Although no other headless myosins have been characterized in vertebrates, there are two examples of such proteins in invertebrates. The use of an alternative promotor in *Drosophila melanogaster* muscle myosin leads to the transcription of a headless myosin, known as myosin related protein (MRP) (Standiford et al., 1997). This protein consists almost entirely of coiled coil and can co-assemble into thick filaments. Similarly, use of an alternative promotor in a molluscan myosin II gene leads to the transcription of catchin, a rod-like protein found in catch muscles (Yamada et al., 2000). In both of these examples, the exons that contain initiation methionine codons are found within large introns of the corresponding muscle myosin genes, and both proteins contain unique N-terminal domains. Although headless Myo10 does not appear to contain any unique N-terminal protein sequence and is not predicted to form a rod-like protein, these examples do set a precedent for the use of alternative transcription start sites to generate headless myosins.

Consistent with the northern blotting data presented here, Yonezawa et al. detected a ~9 kb full-length Myo10 transcript in northern blots of mouse tissues probed with head domain sequence (Yonezawa et al., 2000). However, they also reported as data not shown an additional transcript at ~7 kb, when the blots were probed with sequence from the tail domain. Although the headless transcript we describe here is the first alternative Myo10 transcript characterized to date, the large size of Myo10 raises the possibility that other alternative transcripts may also be produced. Indeed, database searches reveal a 5880 nt cDNA from adult mouse brain (gi:28972398/mKIAA0799) and an EST from embryonic mouse head (gi:46863450), indicating the existence of a slightly shorter form of headless Myo10. This slightly shorter transcript includes the same 5′ UTR found in the headless Myo10 described above, and is identical to it except for skipping the first two protein-coding exons. Translation of this slightly shorter transcript from M_{747} would yield a 151,551 Da (1325 aa) headless Myo10 that includes the IQ motifs and all of the other tail domains found in the headless Myo10 described above.

Based on headless Myo10's domain structure of three IQ motifs, a short segment of coiled coil, three PEST regions, three PH domains, a MyTH4 domain and a FERM domain, we predict that – like full-length Myo10 – headless Myo10 has calmodulin-like light-chains, probably forms a dimer, is susceptible to calpain cleavage, and can bind to PtdIns(3,4,5)P_3, microtubules and integrins. A possible role for headless Myo10 is to act as a natural 'dominant negative' to suppress or spatially limit the activities of full-length Myo10 in neurons. In this regard it should be noticed that a Myo10-tail construct consisting of the PH, MyTH4 and FERM domains appears to act as a dominant-negative inhibitor of phagocytosis in macrophages (Cox et al., 2002). It is also possible that the combination of PH, MyTH4 and FERM domains found in headless Myo10 has functions of its own that are independent of the Myo10 motor domain. Consistent with this possibility, humans express three proteins, MAX-1, PLEKHH2 and FLJ21019, that have domain structures similar to the tail of Myo10 (Fig. 8). Although little is known about PLEKHH2 and FLJ21019, *Caenorhabditis elegans* motor axon guidance-1 (MAX-1) is required for proper guidance of motor neurons through the netrin signaling pathway (Huang et al., 2002).

Expression and localization of Myo10 in brain

Our immunofluorescence experiments clearly show that Myo10 is expressed in neurons, such as Purkinje cells, and in non-neuronal cells, such as astrocytes and ependymal cells. Within Purkinje cells, anti-Myo10 stains cell bodies, dendrites
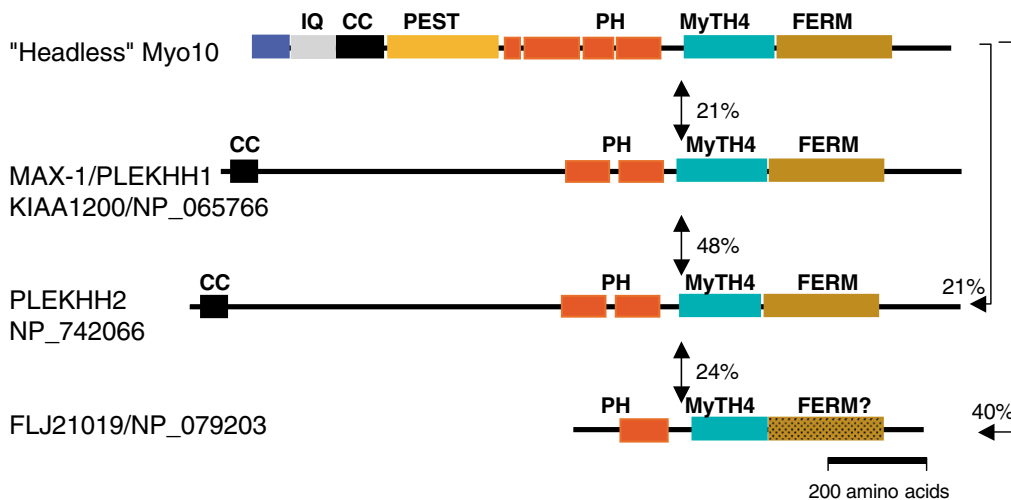

Fig. 8. Diagrams of proteins with domain structures similar to the tail of Myo10. Illustrated are the domain structures of human proteins that are structurally similar to headless Myo10. Domain predictions were based on the NCBI/CDD and/or PFAM servers. Regions predicted to form coiled coils by the PAIRCOIL server are indicated by 'CC'. Arrows indicate protein identity in %. Although the C-terminal portion of FLJ21019 was not recognized as a FERM domain by CDD or PFAM, database searches with FLJ21019 show that it shares 32% protein identity with the FERM domain of Myo10.

and axons. This staining is almost certainly due to full-length Myo10 because only full-length Myo10 was detected in adult cerebellum. The detection of headless Myo10 in cerebrum but not most other tissues suggests that headless Myo10 is expressed primarily in neurons, a conclusion that is also supported by our immunoblots, showing that neuronal cell lines, such as CAD cells express headless Myo10. Further supporting this conclusion is the observation that we have not detected the ~165 kDa headless Myo10 band in a variety of non-neuronal cell lines we have tested by immunoblotting, including HeLa, HEK 293, COS-7, A-431, Swiss 3T3, HL-60, RAW 264.7 and LLC-PK1 cells, all of which do express full-length Myo10.

Developmental regulation of Myo10

The immunoblotting experiments reported here reveal that Myo10 exhibits dramatic developmental regulation in brain. In mouse cerebrum, full-length and headless Myo10 appear to be expressed at roughly similar levels and exhibit a peak of expression between postnatal days 5-15, with much lower expression levels in the adult. Although many different developmental processes occur during this early postnatal period – including process outgrowth and synapse formation – the close link between full-length Myo10 and filopodia suggests that Myo10 is associated with the numerous filopodia generated at this time (Fiala et al., 1998; Ziv and Smith, 1996), when pyramidal neurons are estimated to generate 50,000 dendritic filopodia per day (Portera-Cailliau et al., 2003). Although the roles of myosins in brain are still being worked out (Brown and Bridgman, 2004), Myo1b/myosin-Iα localizes to growth cones (Lewis and Bridgman, 1996), non-muscle myosin-II is required for normal growth cone motility and outgrowth (Brown and Bridgman, 2003; Wylie and Chantler, 2001), and Myo16/Myr8 exhibits a dramatic peak of expression in the first two weeks after birth (Patel et al., 2001). For Myo10, it is important to notice that the expression pattern in cerebrum differs significantly from the one in cerebellum, which expresses relatively little headless Myo10. In addition, expression of full-length Myo10 increases throughout cerebellar development and is highest in adult mice. This expression of Myo10 in adult cerebellum is consistent with our previous in-situ hybridization data (Berg et al., 2000) and our current immunolocalization data in Purkinje cells.

The developmental regulation of Myo10 in brain is particularly interesting given the recent report that Myo10 is one of approximately 20 genes whose expression increased sevenfold or more after a peripheral nerve crush (Tanabe et al., 2003). Northern blots of developing mouse dorsal-root ganglia showed that both the full-length ~9 kb transcript and the shorter ~7 kb transcript were expressed at postnatal day 3, and then declined to lower levels in the adult (Tanabe et al., 2003). When DRG neurons were actively regenerating 7 days after a crush injury, however, both transcripts were significantly upregulated. Together with our results, these data suggest that Myo10 probably plays important roles in the development and regeneration of the nervous system.

Localization of Myo10 in CAD cells

The localization data in CAD cells show that endogenous Myo10 exhibits a striking localization to the tips of filopodia in undifferentiated CAD cells. In addition to tip staining,

however, endogenous Myo10 in undifferentiated CAD cells also exhibits a more diffuse staining of the cell body and cytoplasm. Since transfection of these cells with full-length GFP-Myo10 yields a filopodial-tip pattern, whereas transfection with headless GFP-Myo10 yields a more diffuse localization to the cell body and cytoplasm, we interpret the staining pattern of endogenous Myo10 as the sum of filopodial-tip staining due to full-length Myo10 and a more diffuse staining due largely to headless Myo10.

Immunofluorescence in differentiated CAD cells and rat cortical neurons demonstrated that Myo10 is present at the tips of neuronal filopodia, as well as in growth cones, neurites and neuronal cell bodies. Transfection experiments demonstrated that only full-length Myo10 localizes to the tips of filopodia, whereas headless Myo10 exhibits a more diffuse localization in neurites and cell bodies. This demonstrates that the Myo10 motor is necessary for tip localization in neuronal filopodia and supports the hypothesis that Myo10 uses its own motor activity to transport itself to the tips of filopodial actin bundles.

Dynamics of Myo10 in CAD cells

Live-cell imaging in CAD cell also reveals several important findings related to the movements and functions of Myo10. First, full-length Myo10, but not headless Myo10, localizes to the tips of neuronal filopodia and can undergo intrafilopodial motility. Second, the largely tailless HMM-Myo10 construct behaves similar to full-length Myo10 in that it localizes to the tips of neuronal filopodia and can undergo rearward movements on filopodial actin bundles. This demonstrates that the Myo10 head, neck and coiled coil are sufficient to allow rearward movement, consistent with the hypothesis that rearward movement is due to a rigor-like binding of the Myo10 head domain to actin filaments undergoing retrograde flow. Third, Myo10 can undergo retrograde movements on the filopodial rootlets within lamellipodia, which demonstrates that Myo10 is capable of localizing to portions of filopodia not completely ensheathed by plasma membrane. Fourth, Myo10 was observed at the tips of intrapodia-like processes undergoing 'rocketing' movements. Although this is the first observation associating Myo10 with actin-based rocketing, like that of *Listeria*, it is not unexpected given the overall similarities between intrapodia (Rochlin et al., 1999) and filopodia. Finally, full-length Myo10 localizes to the tips of filopodia at sites of cell-substrate and cell-cell contact. Although this might simply reflect the presence of full-length Myo10 at the tips of virtually all filopodia, Myo10 can bind to β-integrins (Zhang et al., 2004) and filopodia are reported to mediate certain forms of cell-cell contact (Vasioukhin et al., 2000).

Lateral movements of Myo10 along the leading edge and a role for Myo10 at filopodial tips

We have also identified a novel form of Myo10 movement, in which puncta of Myo10 were shown to move laterally along the leading edge of lamellipodia. Kymographic analysis shows that these movements lead tip puncta to collide and undergo lateral fusion events. The actin bundles and filopodial rootlets of growth-cone lamellipodia have been observed to undergo similar lateral movements, and these movements are hypothesized to arise from the lateral pushing forces generated by actin filaments that are polymerizing at angles other than

90° to the leading edge (Katoh et al., 1999a; Katoh et al., 1999b; Oldenbourg et al., 2000). Our observation that small puncta of Myo10 appear along the leading edge and eventually fuse to form larger tip puncta demonstrates that puncta of Myo10 are continuously being 'born' along the leading edge, and that even large and apparently stable tip complexes are actually dynamic structures. Since Myo10 localizes to the tips of filopodial actin bundles – the sites of filopodial actin polymerization – it is probable that Myo10 and the associated filopodial tip complex function in this process. In this regard, it should be noted that neuronal growth cones are reported to have peripheral actin arrays with very prominent filopodial actin bundles and relatively little ARP2/3 at their leading edge (Strasser et al., 2004).

The lateral fusion events of Myo10 puncta in CAD cells also appear closely related to 'Λ-precursors' – the proposed sites of filopodial initiation in the convergent elongation model (Svitkina et al., 2003). Λ-precursors form when actin filaments at the leading edge move laterally, collide and associate at their barbed ends to form Λ-shaped structures that appear to initiate filopodial actin bundles. Since puncta of Myo10 undergo similar movements at the leading edge and form puncta at the tips of actin bundles, Myo10 is probably a component of Λ-precursors and might thus be involved in filopodial initiation. We have previously demontrated an important role for Myo10 in filopodia by showing that GFP-Myo10 can be detected at the tips of filopodia as soon as they form, and by showing that overexpression of Myo10 leads to increased numbers of filopodia (Berg and Cheney, 2002).

In conclusion, we have shown here that brain expresses a headless form of Myo10 that is developmentally regulated but lacks motor activity and does not localize to filopodia. We have also shown that full-length Myo10 undergoes novel forms of movement in neuronal cells, but that headless Myo10 neither localizes to filopodia nor undergoes these movements. These results support the model that Myo10's motor activity is required for its tip localization and intrafilopodial motility. As a molecular motor that binds integrins, Myo10 is also a strong candidate to act as a molecular clutch, whose motor activity can maintain its localization at the tips of growing actin filaments, while its tail provides a link to the cytoplasmic domains of substrate-attached cell-surface molecules. Although the precise functions of headless Myo10 and structurally similar proteins, such as MAX-1, are not yet clear, the localization and dynamics of full-length Myo10 suggests that it functions as a component of a filopodial-tip complex, involved in processes such as filopodial extension and adhesion in developing neurons.

Materials and Methods
Northern blotting and RT-PCR of a headless Myo10 transcript
Probes for northern blotting were generated by PCR. A 366 nt-long probe, specific for full-length Myo10 corresponding to nucleotides 226-591 of human Myo10 cDNA NM_012334 was generated using forward primer 5′-GATAACTT-CTTCACCGAGGGAACAC and reverse primer 5′-CCGGCTGTACTGCTCCAT-GGTGGCAG. A 158 nt-long probe, specific for the putative 5′UTR of headless Myo10 corresponding to nucleotides 33-190 of human EST AI878891 was generated using forward primer 5′-CAGCACAGCCCGAGACGCAC and reverse primer 5′-CTTGGGTTTTCTTTCACCCCTTCAG. A ~1.1 kb probe corresponding to nucleotides 6240-7330 of human Myo10 cDNA NM_012334 reacts with both full-length- and headless-Myo10, as described in Berg et al. (Berg et al., 2000). The human multiple tissue northern blot (Clontech) previously used with this probe was stripped according to the manufacturer's instructions and reprobed essentially as described (Berg et al., 2000).

Reverse transcription (RT)-PCR with Poly A+ mRNA from human brain (Clontech) was used to verify the existence of the headless mRNA predicted by sequence analysis. RT was performed using SuperScript II polymerase (Gibco) according to the manufacturer's instructions, with 1/10 of the RT reaction (2 μl) used for each PCR reaction. The forward primer 5′-CAGCACAGCCCGA-GACGCAC corresponds to nucleotides 33-55 of human EST AI878891, located within the putative headless-specific exon that contains the alternative 5′ UTR. The reverse primer 5′-CTCGCTGTTGGAGGCATCATAGA corresponds to nucleotides 2307-2370 of the full length Myo10, located 377 nucleotides downstream in a protein-coding exon predicted to be present in both headless- and full-length-Myo10. The 377 nt-long PCR product was purified from an agarose gel, cloned into pCRII-TOPO (Invitrogen), and verified by sequencing.

Antibodies and plasmids
An antibody (no. 3568) to the coiled-coil region of mouse Myo10 was raised in chicken as described below. The coiled-coil region (aa 808-918 of mouse Myo10 sequence NP_062345.1) was amplified by PCR using forward primer 5′-CGCGGATCCTACAGGCAGCTGTTGG and reverse primer 5′-CCAAGCTTA-CAGCTTCTGCAGGGA. The PCR product was subcloned into pQE-30 vector (Qiagen) using restriction sites engineered into the PCR primers. The resulting 123 aa RGS-His tagged fusion protein was expressed in the XL1-blue strain of *Escherichia coli*, solubilized in 20 mM Tris pH 8.0 with 500 mM NaCl buffer and purified by two cycles of absorption-elution on Ni-NTA agarose resin (Qiagen) followed by anion-exchange chromatography on Q-Sepharose Fast Flow resin (Pharmacia). This fusion protein was injected into a chicken and the IgY from eggs (Aves Labs) was purified on an affinity column consisting of the coiled-coil fusion protein. Full-length GFP-Myo10 (aa 1-2052 of bovine Myo10 sequence U55042), GFP-Myo10-HMM (aa 1-943) and a GFP-tagged construct corresponding to the headless form of Myo10 (aa 644-2052) were generated in pEGFP-C2 as previously described (Berg and Cheney, 2002).

Tissue samples and immunoblotting
To determine the developmental expression pattern of Myo10, brains from a litter of C57/black mice were collected at different time points, dissected into cerebri and cerebelli and frozen in liquid nitrogen until all time points had been collected. Samples were homogenized in 10 ml/g of Lysis Buffer (1×PBS with 5 mM DTT, 1 mM Pefabloc, 5 μg/ml pepstatin A, 5 μg/ml leupeptin, 2 mM EDTA, 0.2 mM PMSF and 1% Sigma protease inhibitor cocktail cat. no. P-8440) and boiled immediately in SDS sample buffer. Immunoblotting was performed as described previously (Berg et al., 2000), except that 1 μg/ml of Myo10 antibody no. 3568 was used here.

Cell culture and transfection
CAD cells are a subclone of Cath-a cells that can be differentiated into a catecholaminergic neuronal phenotype by serum withdrawl (Qi et al., 1997). CAD cells were cultured in HAM-F12 with 8% fetal bovine serum (FBS) and 1% penicillin/streptomycin as previously described (Wang and Oxford, 2000). Undifferentiated CAD cells were transiently transfected at 60-80% confluence using Polyfect (Qiagen) for 12 hours following to the manufacturer's instructions for HeLa cells. CAD cell differentiation was induced 1 day after transfection by 1-3 days of serum withdrawal. Lysates were prepared by scraping cells in Lysis Buffer and homogenizing on ice with ~75 strokes of a Dounce homogenizer.

Staining procedures
For immunofluorescence, CAD cells were plated onto coverslips that had been coated with 20 μg/ml laminin (Invitrogen). Cells were fixed with 4% paraformaldehyde for 10 minutes, permeabilized with 0.2% Triton X-100 for 5 minutes, blocked with 5% heat-inactivated goat serum for 1 hour in PBS and washed three times for 15 minutes in PBS. Coverslips were then incubated overnight at 4°C with 1 μg/ml of chicken anti-Myo10 antibody no. 3568 or chicken non-immune IgG in PBS plus goat serum, rinsed three times in PBS, and incubated 1-3 hour at room temperature with 0.5 μg/ml goat anti-chicken secondary antibody (Molecular Probes, no. A-11039) in PBS plus goat serum. Coverslips were then incubated with 1.5 nM rhodamine-phalloidin and 30 nM DAPI in PBS for 0.5 hour, washed three times in PBS, and mounted in Gel/Mount (Biomeda).

30-μm-thick cryo-sections of brain for immunofluorescence were obtained from P70 mice, and were then perfused with 50 ml saline buffer and 50 ml 4% paraformaldehyde followed by immersion at 4°C in 4% paraformaldehyde overnight and 30% sucrose in 0.1 M phosphate buffer (pH 7.4) for 2-3 days. Floating sections were permeabilized with three washes of PBSX (PBS plus 0.2% Triton X-100), incubated 1 hour at room temperature in blocking buffer (PBSX plus 5% BSA and 1% goat serum; filtered through a 0.2 μm filter) and incubated overnight at 4°C with primary antibodies in blocking buffer. Chicken anti-Myo10 antibody no. 3568 and a non-immune chicken IgG control were used at 4 μg/ml, whereas rabbit anti-calbindin (Sigma, no. C-2724) and rabbit anti-GFAP (Chemicon no. AB5804) were used at 1:500 dilution. Sections were washed three times with PBSX, incubated for 1 hour with secondary antibodies (Molecular Probes, nos A-11039 and A-11011)

at 8 μg/ml in Blocking Buffer, washed three times with PBSX, and mounted with Vectashield (Vector labs).

Imaging and analysis

Brain sections were imaged with a Zeiss Axioplan2 confocal microscope with a BioRad Radiance 2000 scanning system using either a 10× or 1.4 NA 63× lens. Cultured cells were imaged using a wide-field inverted microscope with a cooled CCD and Metamorph software. Time-lapse images were acquired in phase and fluorescence every 5 seconds for 3-60 minutes using exposure times of 100-600 mseconds at 37°C with a 60× 1.4 NA lens. To separate CFP and GFP images in double-labeled cells, images were captured using a Chroma 86006bs beamsplitter with an excitation filter wheel (CFP: 431-441 nm; GFP: 483-501 nm) and an emission filter wheel (CFP: 450-490 nm; GFP: 520-550 nm). Immunfluorescence images and their corresponding controls were collected and scaled identically for brightness and contrast with Metamorph or Adobe Photoshop. Kymographs of the leading edge were generated with Metamorph to outline the edge of a cell and plotting the maximum brightness-value from a line-width of 13 pixels.

References

Belyantseva, I. A., Boger, E. T. and Friedman, T. B. (2003). Myosin XVa localizes to the tips of inner ear sensory cell stereocilia and is essential for staircase formation of the hair bundle. *Proc. Natl. Acad. Sci. USA* **100**, 13958-13963.

Berg, J. S. and Cheney, R. E. (2002). Myosin-X is an unconventional myosin that undergoes intrafilopodial motility. *Nat. Cell Biol.* **4**, 246-250.

Berg, J. S., Derfler, B. H., Pennisi, C. M., Corey, D. P. and Cheney, R. E. (2000). Myosin-X, a novel myosin with pleckstrin homology domains, associates with regions of dynamic actin. *J. Cell Sci.* **113**, 3439-3451.

Berg, J. S., Powell, B. C. and Cheney, R. E. (2001). A millennial myosin census. *Mol. Biol. Cell* **12**, 780-794.

Brown, M. E. and Bridgman, P. C. (2003). Retrograde flow rate is increased in growth cones from myosin IIB knockout mice. *J. Cell Sci.* **116**, 1087-1094.

Brown, M. E. and Bridgman, P. C. (2004). Myosin function in nervous and sensory systems. *J. Neurobiol.* **58**, 118-130.

Burge, C. and Karlin, S. (1997). Prediction of complete gene structures in human genomic DNA. *J. Mol. Biol.* **268**, 78-94.

Cox, D., Berg, J. S., Cammer, M., Chinegwundoh, J. O., Dale, B. M., Cheney, R. E. and Greenberg, S. (2002). Myosin X is a downstream effector of PI(3)K during phagocytosis. *Nat. Cell Biol.* **4**, 469-477.

Davenport, R. W., Dou, P., Rehder, V. and Kater, S. B. (1993). A sensory role for neuronal growth cone filopodia. *Nature* **361**, 721-724.

Fiala, J. C., Feinberg, M., Popov, V. and Harris, K. M. (1998). Synaptogenesis via dendritic filopodia in developing hippocampal area CA1. *J. Neurosci.* **18**, 8900-8911.

Gerhardt, H., Golding, M., Fruttiger, M., Ruhrberg, C., Lundkvist, A., Abramsson, A., Jeltsch, M., Mitchell, C., Alitalo, K., Shima, D. et al. (2003). VEGF guides angiogenic sprouting utilizing endothelial tip cell filopodia. *J. Cell Biol.* **161**, 1163-1177.

Homma, K., Saito, J., Ikebe, R. and Ikebe, M. (2001). Motor function and regulation of myosin X. *J. Biol. Chem.* **276**, 34348-34354.

Huang, X., Cheng, H. J., Tessier-Lavigne, M. and Jin, Y. (2002). MAX-1, a novel PH/MyTH4/FERM domain cytoplasmic protein implicated in netrin-mediated axon repulsion. *Neuron* **34**, 563-576.

Isakoff, S. J., Cardozo, T., Andreev, J., Li, Z., Ferguson, K. M., Abagyan, R., Lemmon, M. A., Aronheim, A. and Skolnik, E. Y. (1998). Identification and analysis of PH domain-containing targets of phosphatidylinositol 3-kinase using a novel in vivo assay in yeast. *EMBO J.* **17**, 5374-5387.

Jay, D. G. (2000). The clutch hypothesis revisited: ascribing the roles of actin-associated proteins in filopodial protrusion in the nerve growth cone. *J. Neurobiol.* **44**, 114-125.

Johansson, C. B., Momma, S., Clarke, D. L., Risling, M., Lendahl, U. and Frisen, J. (1999). Identification of a neural stem cell in the adult mammalian central nervous system. *Cell* **96**, 25-34.

Katoh, K., Hammar, K., Smith, P. J. and Oldenbourg, R. (1999a). Arrangement of radial actin bundles in the growth cone of Aplysia bag cell neurons shows the immediate past history of filopodial behavior. *Proc. Natl. Acad. Sci. USA* **96**, 7928-7931.

Katoh, K., Hammar, K., Smith, P. J. and Oldenbourg, R. (1999b). Birefringence imaging directly reveals architectural dynamics of filamentous actin in living growth cones. *Mol. Biol. Cell* **10**, 197-210.

Lewis, A. K. and Bridgman, P. C. (1996). Mammalian myosin I alpha is concentrated near the plasma membrane in nerve growth cones. *Cell Motil. Cytoskeleton* **33**, 130-150.

Lin, C. H., Espreafico, E. M., Mooseker, M. S. and Forscher, P. (1997). Myosin drives retrograde F-actin flow in neuronal growth cones. *Biol. Bull.* **192**, 183-185.

Mallavarapu, A. and Mitchison, T. (1999). Regulated actin cytoskeleton assembly at filopodium tips controls their extension and retraction. *J. Cell Biol.* **146**, 1097-1106.

Mashanov, G. I., Tacon, D., Peckham, M. and Molloy, J. E. (2004). The spatial and temporal dynamics of pleckstrin homology domain binding at the plasma membrane measured by imaging single molecules in live mouse myoblasts. *J. Biol. Chem.* **279**, 15274-15280.

Mitchison, T. and Kirschner, M. (1988). Cytoskeletal dynamics and nerve growth. *Neuron* **1**, 761-772.

Oldenbourg, R., Katoh, K. and Danuser, G. (2000). Mechanism of lateral movement of filopodia and radial actin bundles across neuronal growth cones. *Biophys. J.* **78**, 1176-1182.

Patel, K. G., Liu, C., Cameron, P. L. and Cameron, R. S. (2001). Myr 8, a novel unconventional myosin expressed during brain development associates with the protein phosphatase catalytic subunits 1alpha and 1gamma1. *J. Neurosci.* **21**, 7954-7968.

Portera-Cailliau, C., Pan, D. T. and Yuste, R. (2003). Activity-regulated dynamic behavior of early dendritic protrusions: evidence for different types of dendritic filopodia. *J. Neurosci.* **23**, 7129-7142.

Qi, Y., Wang, J. K., McMillian, M. and Chikaraishi, D. M. (1997). Characterization of a CNS cell line, CAD, in which morphological differentiation is initiated by serum deprivation. *J. Neurosci.* **17**, 1217-1225.

Rochlin, M. W., Dailey, M. E. and Bridgman, P. C. (1999). Polymerizing microtubules activate site-directed F-actin assembly in nerve growth cones. *Mol. Biol. Cell* **10**, 2309-2327.

Rogers, M. S. and Strehler, E. E. (2001). The tumor-sensitive calmodulin-like protein is a specific light chain of human unconventional myosin x. *J. Biol. Chem.* **276**, 12182-12189.

Rorth, P. (2003). Communication by touch: role of cellular extensions in complex animals. *Cell* **112**, 595-598.

Smith, S. J. (1988). Neuronal cytomechanics: the actin-based motility of growth cones. *Science* **242**, 708-715.

Sousa, A. D. and Cheney, R. E. (2005). Myosin-X: a molecular motor at the cell's fingertips. *Trends Cell Biol.* **15**, 533-539.

Standiford, D. M., Davis, M. B., Miedema, K., Franzini-Armstrong, C. and Emerson, C. P. (1997). Myosin rod protein: a novel thick filament component of Drosophila muscle. *J. Mol. Biol.* **265**, 40-55.

Strasser, G. A., Rahim, N. A., VanderWaal, K. E., Gertler, F. B. and Lanier, L. M. (2004). Arp2/3 is a negative regulator of growth cone translocation. *Neuron* **43**, 81-94.

Suter, D. M. and Forscher, P. (2000). Substrate-cytoskeletal coupling as a mechanism for the regulation of growth cone motility and guidance. *J. Neurobiol.* **44**, 97-113.

Svitkina, T. M., Bulanova, E. A., Chaga, O. Y., Vignjevic, D. M., Kojima, S., Vasiliev, J. M. and Borisy, G. G. (2003). Mechanism of filopodia initiation by reorganization of a dendritic network. *J. Cell Biol.* **160**, 409-421.

Tanabe, K., Bonilla, I., Winkles, J. A. and Strittmatter, S. M. (2003). Fibroblast growth factor-inducible-14 is induced in axotomized neurons and promotes neurite outgrowth. *J. Neurosci.* **23**, 9675-9686.

Titus, M. A. (1999). A class VII unconventional myosin is required for phagocytosis. *Curr. Biol.* **9**, 1297-1303.

Tuxworth, R. I., Weber, I., Wessels, D., Addicks, G. C., Soll, D. R., Gerisch, G. and Titus, M. A. (2001). A role for myosin VII in dynamic cell adhesion. *Curr. Biol.* **11**, 318-329.

Vasioukhin, V., Bauer, C., Yin, M. and Fuchs, E. (2000). Directed actin polymerization is the driving force for epithelial cell-cell adhesion. *Cell* **100**, 209-219.

Wang, H. and Oxford, G. S. (2000). Voltage-dependent ion channels in CAD cells: A catecholaminergic neuronal line that exhibits inducible differentiation. *J. Neurophysiol.* **84**, 2888-2895.

Weber, K. L., Sokac, A. M., Berg, J. S., Cheney, R. E. and Bement, W. M. (2004). A microtubule-binding myosin required for nuclear anchoring and spindle assembly. *Nature* **431**, 325-329.

Wylie, S. R. and Chantler, P. D. (2001). Separate but linked functions of conventional myosins modulate adhesion and neurite outgrowth. *Nat. Cell Biol.* **3**, 88-92.

Yamada, A., Yoshio, M., Oiwa, K. and Nyitray, L. (2000). Catchin, a novel protein in molluscan catch muscles, is produced by alternative splicing from the myosin heavy chain gene. *J. Mol. Biol.* **295**, 169-178.

Yonezawa, S., Kimura, A., Koshiba, S., Masaki, S., Ono, T., Hanai, A., Sonta, S., Kageyama, T., Takahashi, T. and Moriyama, A. (2000). Mouse myosin X: molecular architecture and tissue expression as revealed by northern blot and in situ hybridization analyses. *Biochem. Biophys. Res. Commun.* **271**, 526-533.

Zhang, H., Berg, J. S., Li, Z., Wang, Y., Lang, P., Sousa, A. D., Bhaskar, A., Cheney, R. E. and Stromblad, S. (2004). Myosin-X provides a motor-based link between integrins and the cytoskeleton. *Nat. Cell Biol.* **6**, 523-531.

Zhou, F. Q., Waterman-Storer, C. M. and Cohan, C. S. (2002). Focal loss of actin bundles causes microtubule redistribution and growth cone turning. *J. Cell Biol.* **157**, 839-849.

Ziv, N. E. and Smith, S. J. (1996). Evidence for a role of dendritic filopodia in synaptogenesis and spine formation. *Neuron* **17**, 91-102.